Supplementary Information

A novel epoxy resin-based cathode binder for low cost, long cycling life, and high-energy lithium-sulfur battery

Longlong Yan,[a,b,‡], Xiguang Gao,[b,‡] Farihah Wahid-Pedro,[b] Jesse Thomas Ernest Quinn,[b] Yuezhong Meng *[a] and Yuning Li*[b]

[a.] *The Key Laboratory of Low-Carbon Chemistry & Energy Conservation of Guangdong Province/State Key Laboratory of Optoelectronic Materials and Technologies, School of Materials Science and Engineering, Sun Yat-sen University, Guangzhou 510275, P. R. China.E-mail: mengyzh@sysu.edu.cn*

[b.] *Department of Chemical Engineering and Waterloo Institute for Nanotechnology (WIN) University of Waterloo, 200 University Ave West, Waterloo, Ontario, Canada, N2L 3G1. yuning.li@uwaterloo.ca; Tel: 1-519-888-4567 ext. 31105; Fax: 1-519-888-4347*

Density functional theory (DFT) calculations.

Simulations were performed at the RB3LYP 6-31+G(d,p) level of DFT using Gaussian 09 revision A.02.[1] After confirming by the absence of imaginary frequencies that the stationary points obtained in the geometry optimizations were minima, the adsorption binding energy (E_d) was computed to measure the binding strength of different lithium sulfides, Li_2S, Li_2S_2, Li_2S_3, Li_2S_4, Li_2S_6, and Li_2S_8, with the chelating nitrogen, oxygen, or fluorine atoms of the structural segments of PEI-ER and PVDF. $E_d = E_{Li2Sx} + E_{Polymer\ segment} - E_{Li2Sx+Polymer\ segment}$, where E_{Li2Sx}, $E_{Polymer\ segment}$, and $E_{Li2Sx+Polymer\ segment}$ are the minimized ground-state energies of Li_2S_x, polymer segment, and the complex of Li_2S_x and polymer segment, respectively. The simulated results are shown in Figures S1-S5.
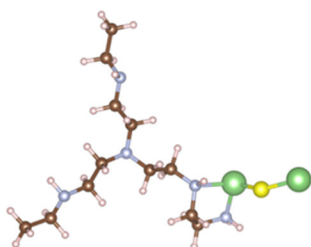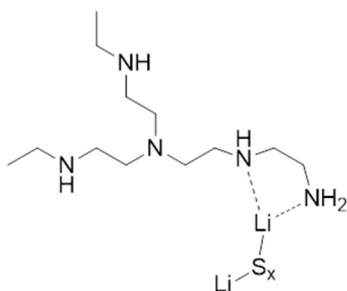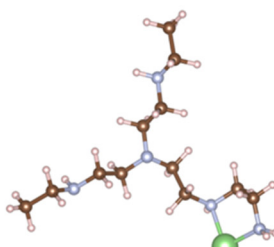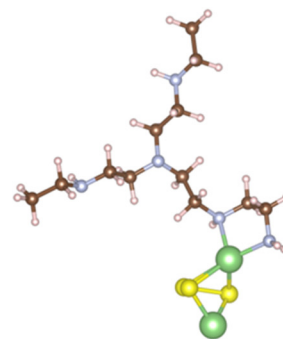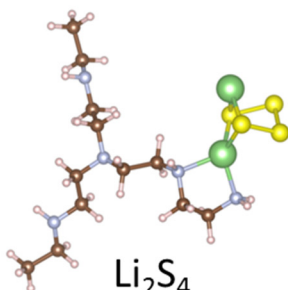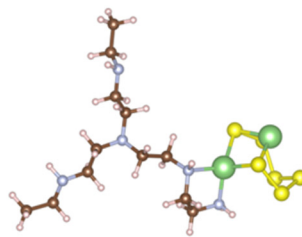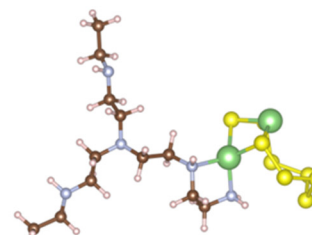
Figure S1. The optimized geometries and adsorption binding energies (E_d's) of the complexes between a PEI segment, PEI-1, in the PEI-ER resin and Li_2S, Li_2S_2, Li_2S_3, Li_2S_4, Li_2S_6, and Li_2S_8 through the interactions of one Li ion with one primary N atom and one adjacent secondary N atom obtained at the RB3LYP 6-31+G(d,p) level of DFT using Gaussian 09 revision A.02.
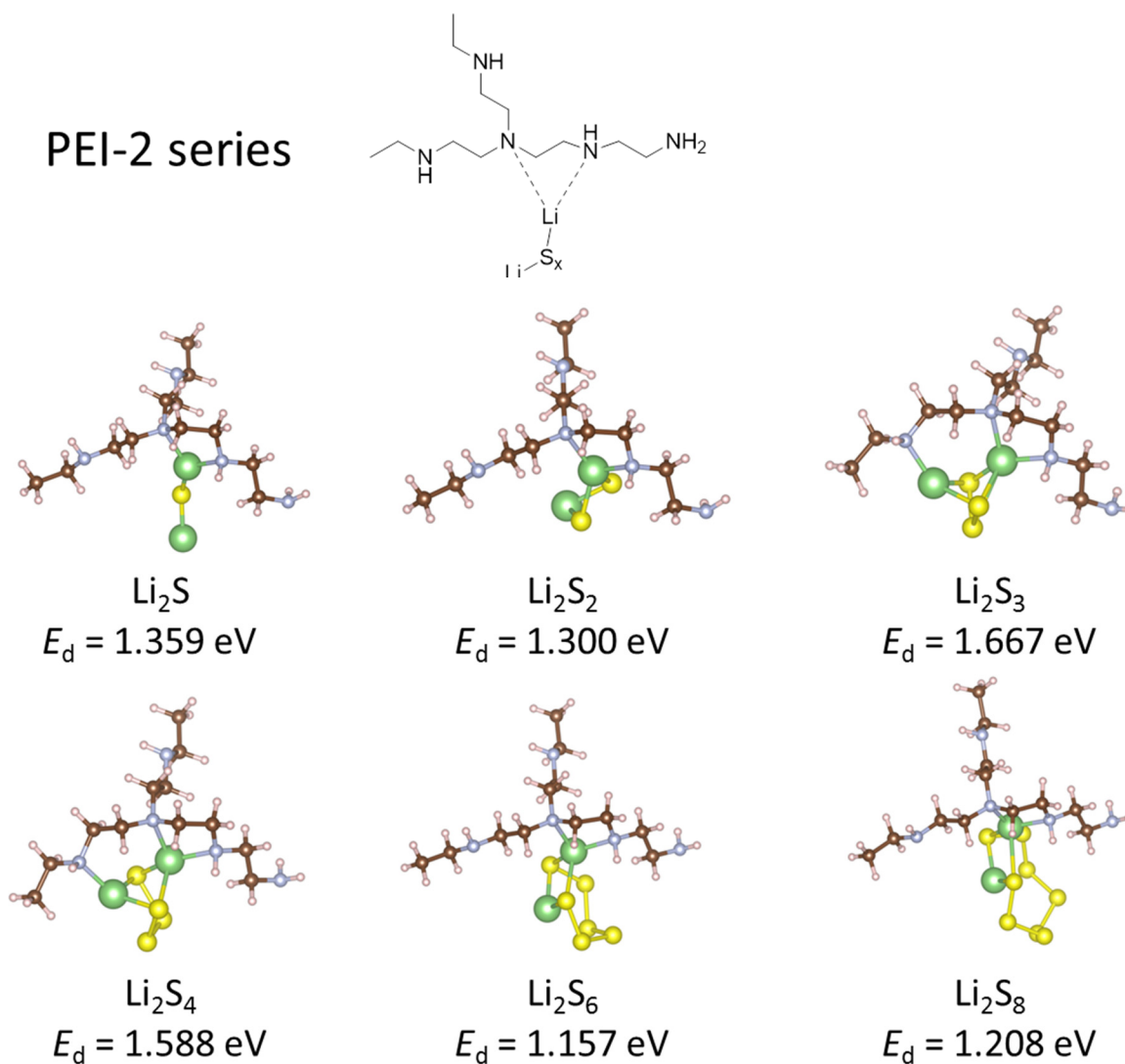
Figure S2. The optimized geometries and adsorption binding energies (E_d's) of the complexes between a PEI segment, PEI-2, in the PEI-ER resin and Li_2S, Li_2S_2, Li_2S_3, Li_2S_4, Li_2S_6, and Li_2S_8 through the interactions of one Li ion with one secondary N atom and one nearby tertiary N atom obtained at the RB3LYP 6-31+G(d,p) level of DFT using Gaussian 09 revision A.02. Note that the Li ion of Li_2S_3 or Li_2S_4 forms an additional binding with a third N atom on the adjacent branch to form a tri-dent complex, resulting in an abnormally high E_d than the rest of lithium sulfides.
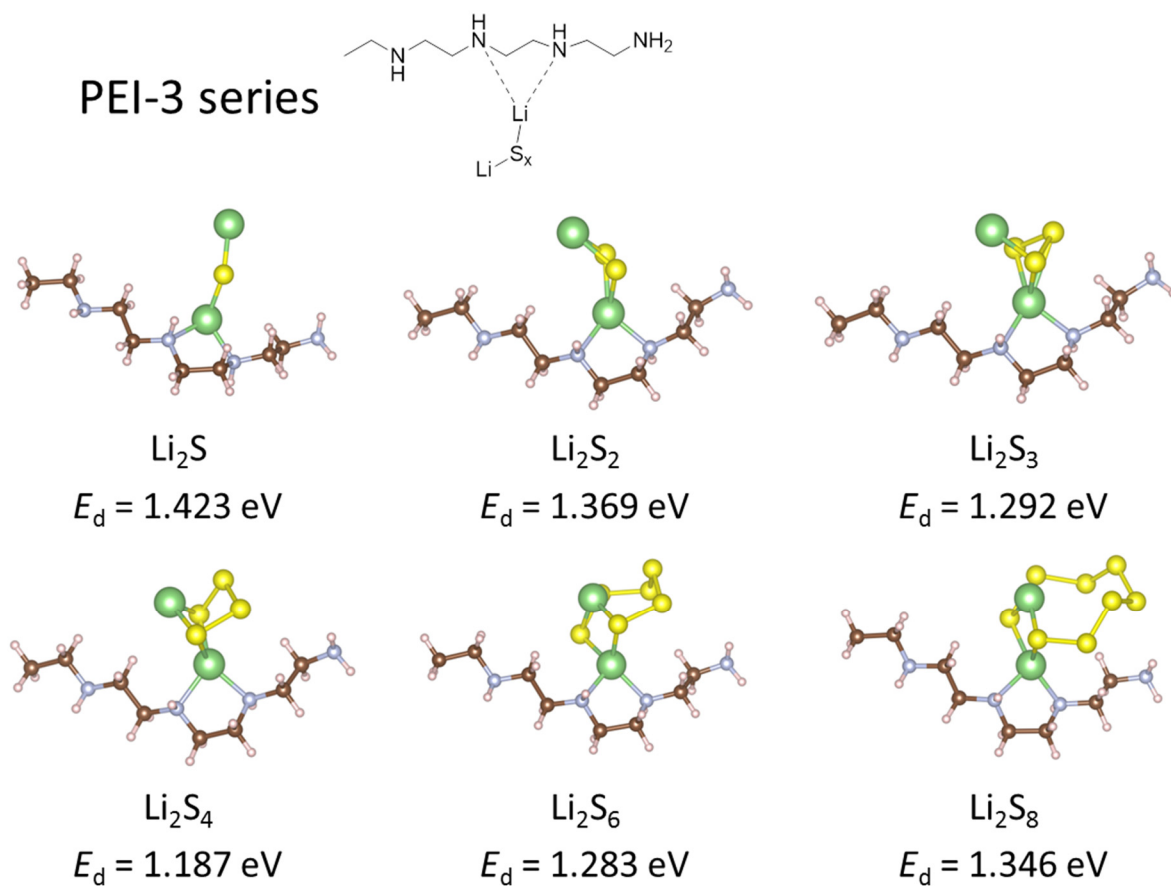
Figure S3. The optimized geometries and adsorption binding energies (E_d's) of the complexes between a PEI segment, PEI-3, in the PEI-ER resin and Li_2S, Li_2S_2, Li_2S_3, Li_2S_4, Li_2S_6, and Li_2S_8 through the interactions of one Li ion with two nearby secondary N atoms obtained at the RB3LYP 6-31+G(d,p) level of DFT using Gaussian 09 revision A.02.
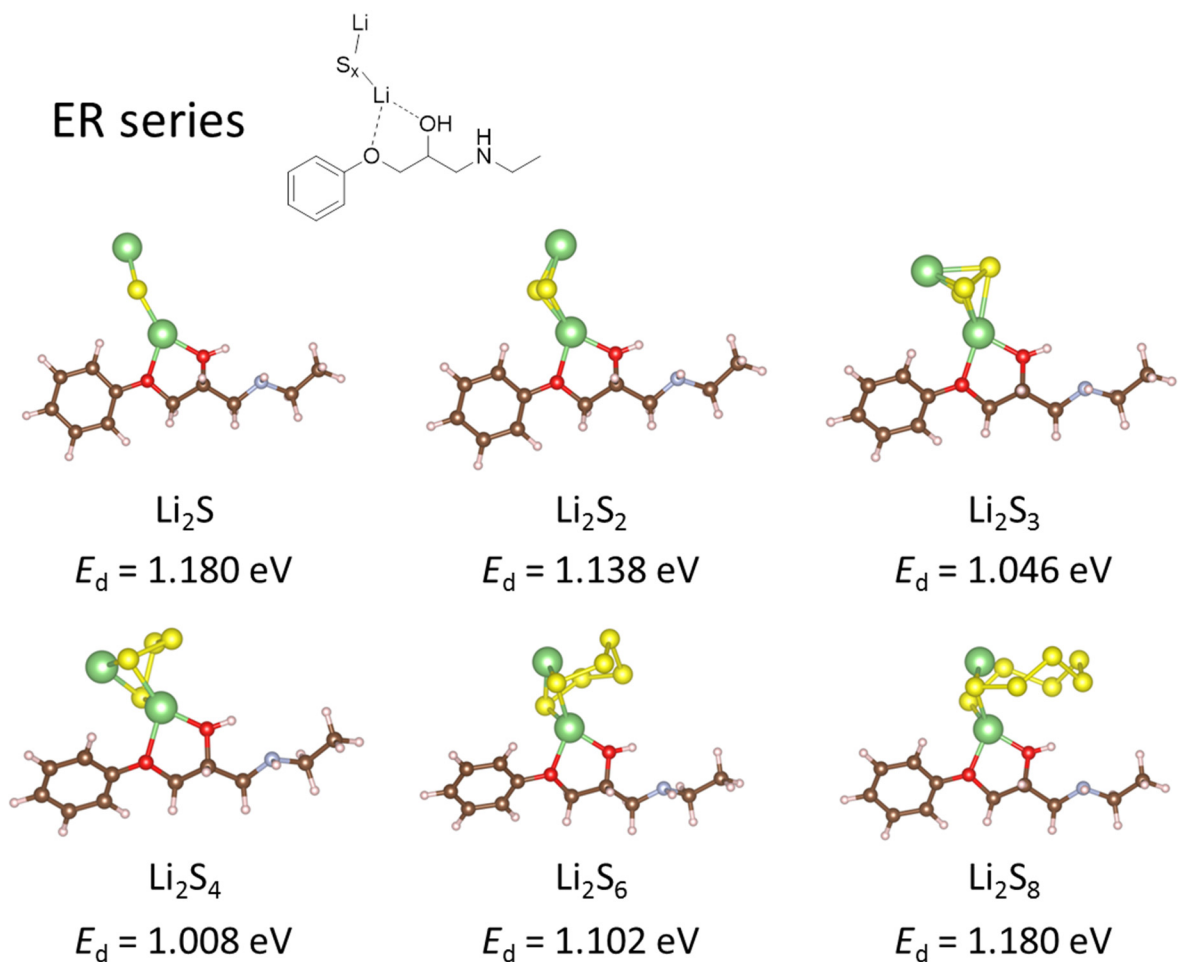
Figure S4. The optimized geometries and adsorption binding energies (E_d's) of the complexes between an ER segment in the PEI-ER resin and Li_2S, Li_2S_2, Li_2S_3, Li_2S_4, Li_2S_6, and Li_2S_8 through the interactions of one Li ion with two nearby O atoms obtained at the RB3LYP 6-31+G(d,p) level of DFT using Gaussian 09 revision A.02.

Figure S5. The optimized geometries and adsorption binding energies (E_d's) of the complexes between a PVDF segment and Li_2S, Li_2S_2, Li_2S_3, Li_2S_4, Li_2S_6, and Li_2S_8 through the interactions of one Li ion with two nearby F atoms obtained at the RB3LYP 6-31+G(d,p) level of DFT using Gaussian 09 revision A.02.
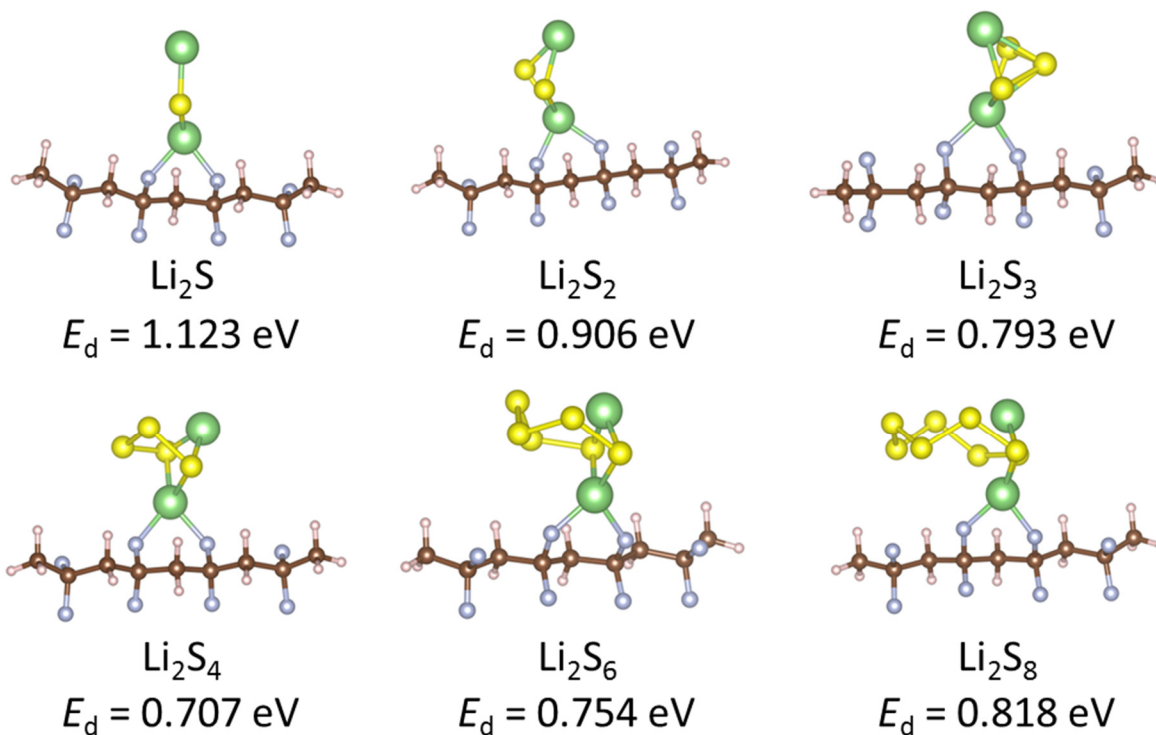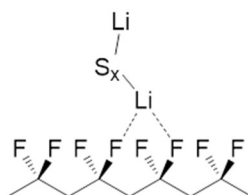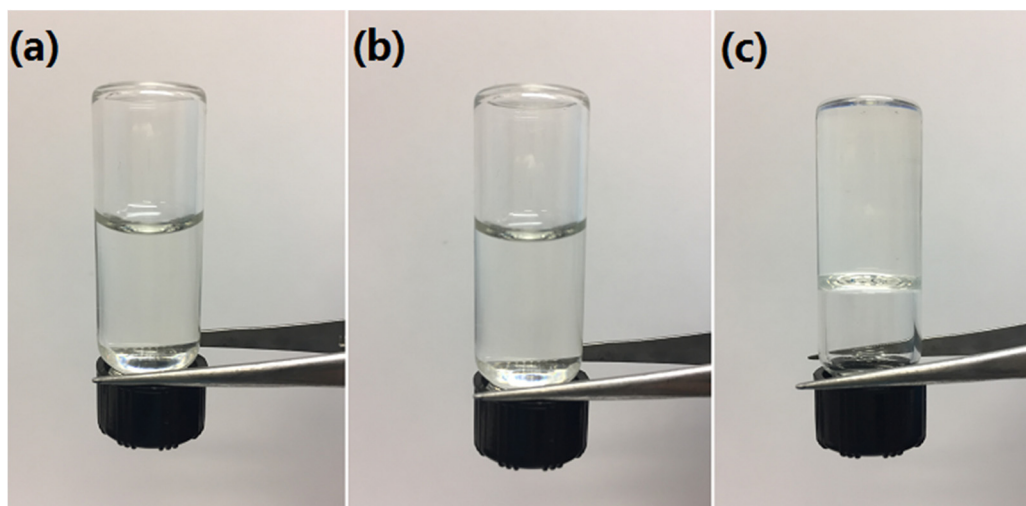
Figure S6. A solution of PEI and ER (weight ratio of 1:2) in NMP after: (a) 24 h, (b) 48 h and (c) 72 h at room temperature. No noticeable increase in viscosity was observed within 48 h, while the viscosity increased significantly after 72 h.
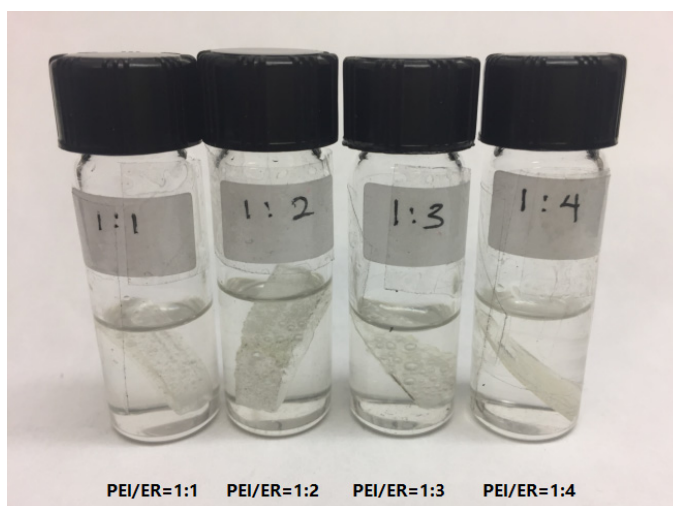

Figure S7. PEI-ER polymer binders soaked in electrolyte solutions after a week. No noticeable deformation was observed.
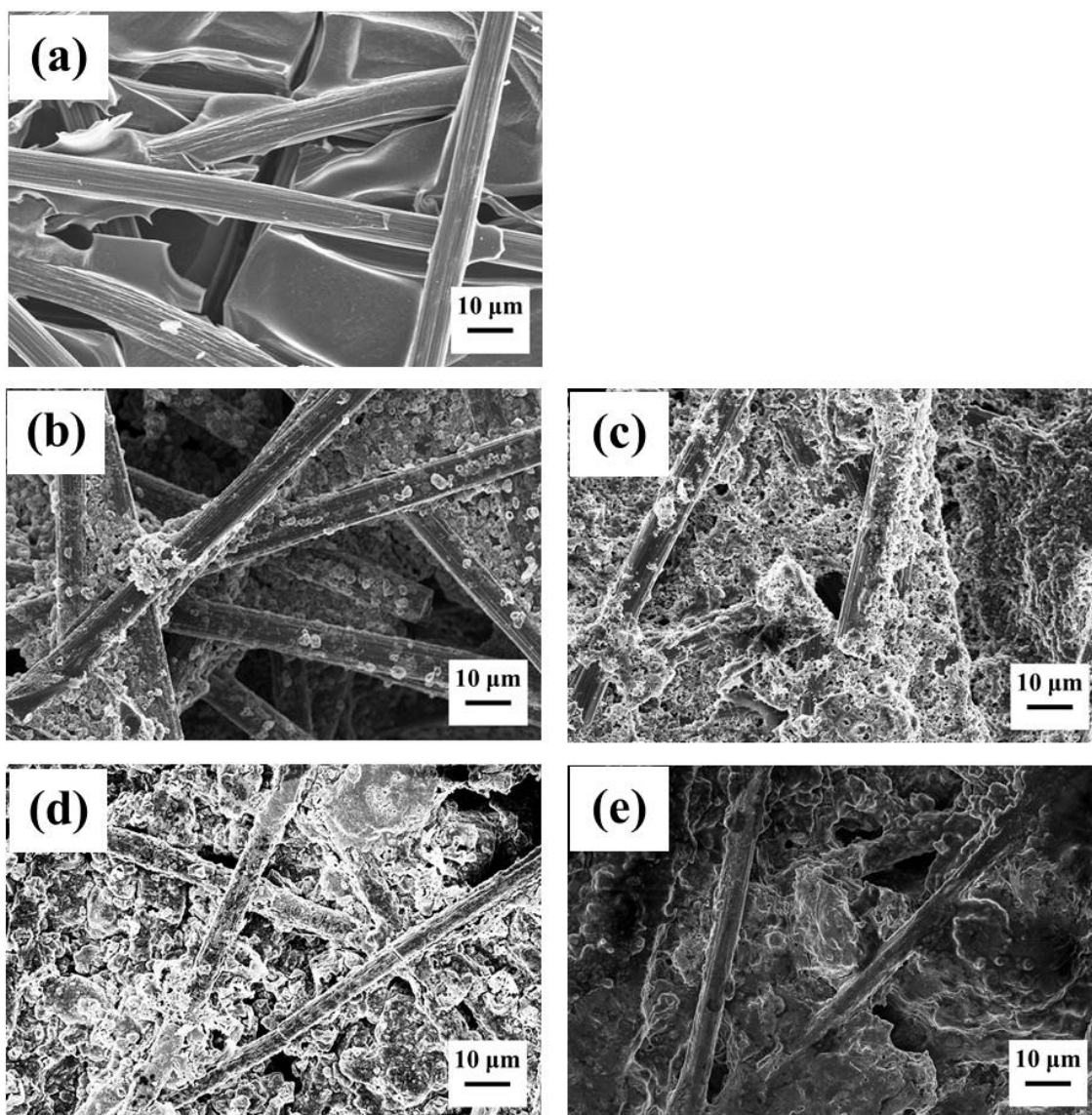
Figure S8. SEM characterization of sulfur cathodes which used the PEI-ER$_{1:2}$ binder with areal sulfur loadings of 1.9 mg cm^{-1} before and after cycling for 1000 cycles in the charged state. (a) Bare carbon paper (CP) current collector. NPS:SP:PEI-ER$_{1:2}$ on CP cathode without the interlayer (IL) structure before cycling (b) and after cycling (d). NPS:SP:PEI-ER$_{1:2}$ on CP cathode with the IL structure before cycling (c) and after cycling (e).
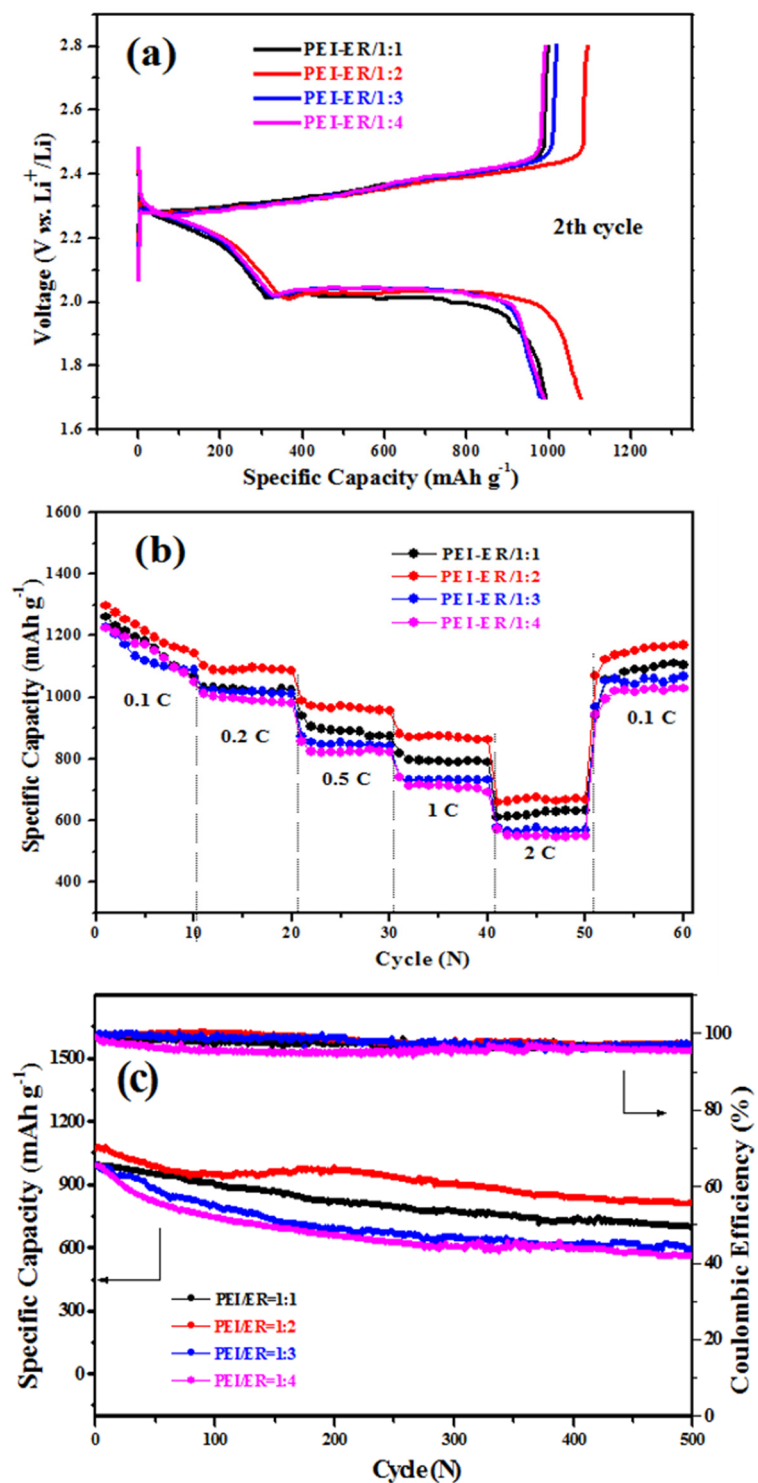
Figure S9. Discharge-charge performance for SS:SP:PEI-ER cathodes (Type A in Figure 2a) with various PEI:ER ratios: (a) voltage *vs*. capacity profiles at 0.5 C during 2nd cycle; (b) rate performance discharged at various C-rates; and (c) long-term cycling performance at 0.5 C in the voltage range of 1.7-2.8 V.
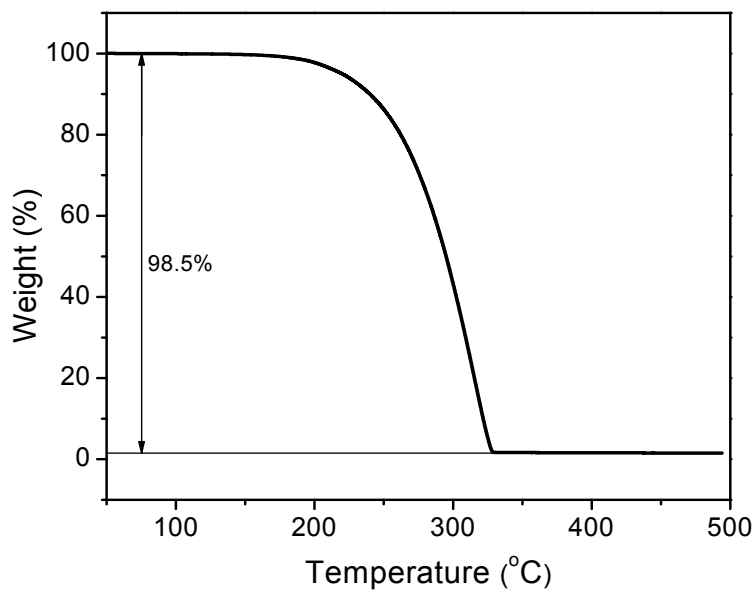
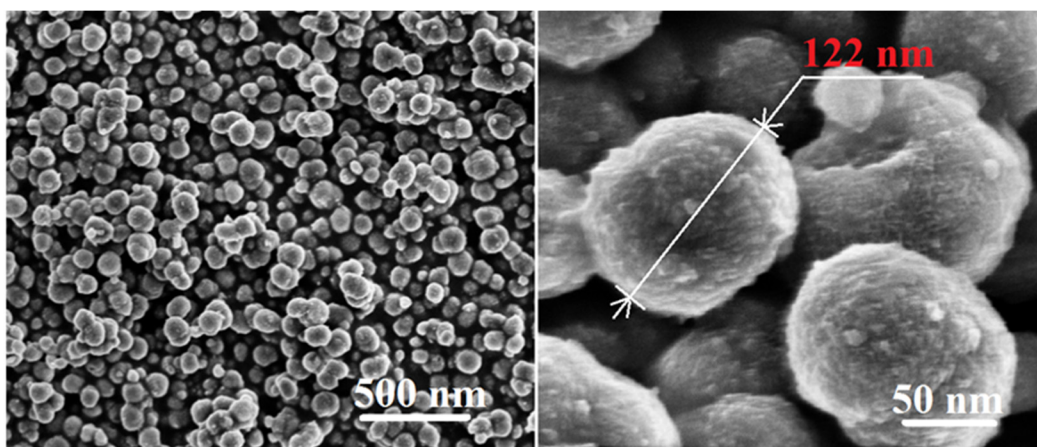**Figure S10.** Thermogravimetric analysis (TGA) of NPS at a heating rate of 20 °C min^{-1} under nitrogen.

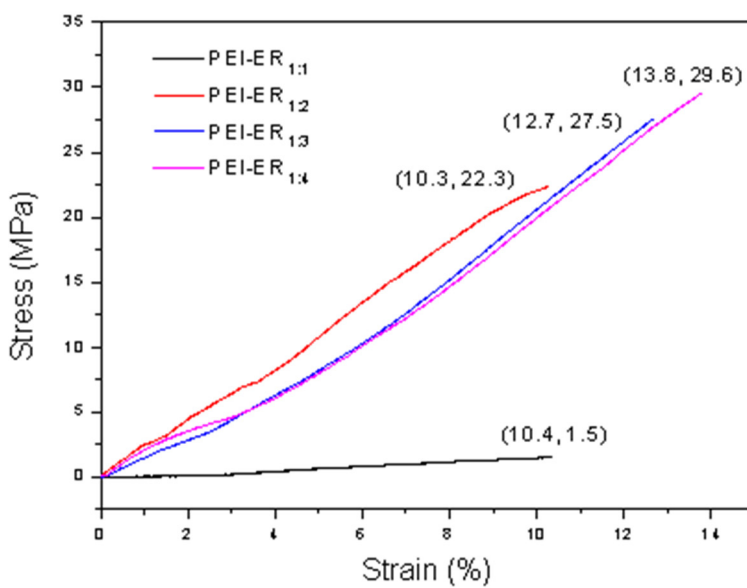**Figure S11.** SEM images of sulfur nanoparticles (NPS).

Figure S12. Stress-strain curves of cross-linked PEI-ER films, which were prepared by cross-linking PEI and ER of different weight ratios at 50 °C under vacuum for 48 h. The films were tested using a universal tensile tester with a gauge length of 14 mm at a cross-head speed of 0.2 mm min^{-1}.
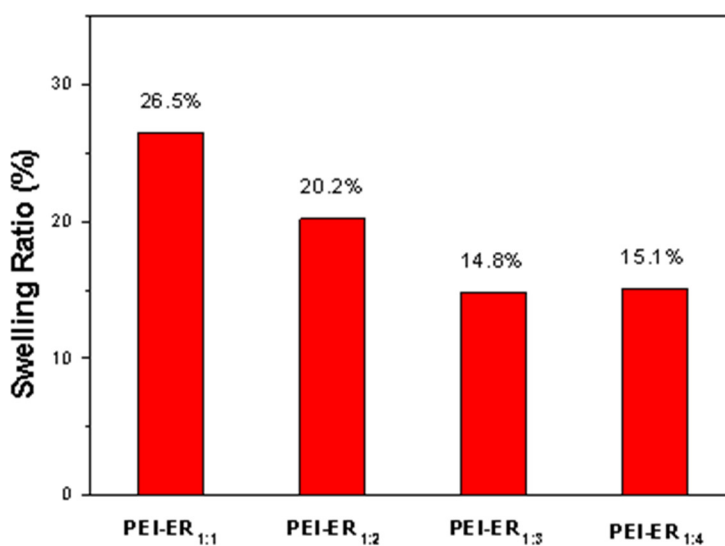

Figure S13. Electrolyte solvent uptakes of PEI-ER binders. Swelling ratio is defined as the weight of electrolyte solvent (DOL/DME, v/v of 1/1) absorbed by the cross-linked PEI-ER film after soaking in the electrolyte solvent for 1 week divided by the weight of polymer film before soaking.

Table S1. Sulfur weight losses of cathode materials after Soxhlet extraction with CS_2.

Samples	Weight		Total weight loss	Sulfur weight loss
	Before Soxhlet extraction	After (n h) Soxhlet extraction		
70%NPS+20%SuperP+10%PVDF	1.0000 g	0.2980 g (5 h)	70.2%	100%
70%NPS+20%SuperP+10%PEI-ER$_{1:2}$	1.0011 g	0.5202 g (5 h)	48.0%	69%
70%NPS+20%SuperP+10%PEI-ER$_{1:2}$	1.0010 g	0.4837 g (48 h)	51.7%	74%

References

1. M. J. Frisch, G. W. Trucks, H. B. Schlegel, G. E. Scuseria, M. A. Robb, J. R. Cheeseman, G. Scalmani, V. Barone, G. A. Petersson, H. Nakatsuji, X. Li, M. Caricato, A. Marenich, J. Bloino, B. G. Janesko, R. Gomperts, B. Mennucci, H. P. Hratchian, J. V. Ortiz, A. F. Izmaylov, J. L. Sonnenberg, D. Williams-Young, F. Ding, F. Lipparini, F. Egidi, J. Goings, B. Peng, A. Petrone, T. Henderson, D. Ranasinghe, V. G. Zakrzewski, J. Gao, N. Rega, G. Zheng, W. Liang, M. Hada, M. Ehara, K. Toyota, R. Fukuda, J. Hasegawa, M. Ishida, T. Nakajima, Y. Honda, O. Kitao, H. Nakai, T. Vreven, K. Throssell, J. A. Montgomery, Jr., J. E. Peralta, F. Ogliaro, M. Bearpark, J. J. Heyd, E. Brothers, K. N. Kudin, V. N. Staroverov, T. Keith, R. Kobayashi, J. Normand, K. Raghavachari, A. Rendell, J. C. Burant, S. S. Iyengar, J. Tomasi, M. Cossi, J. M. Millam, M. Klene, C. Adamo, R. Cammi, J. W. Ochterski, R. L. Martin, K. Morokuma, O. Farkas, J. B. Foresman, and D. J. Fox, Gaussian, Inc., Wallingford CT, Gaussian 09, Revision A.02, 2016.